Band gap engineering of Au doping and Au -N codoping into anatase TiO 2 for enhancing the visible light photocatalytic performance

Mohammed Benali Kanoun, Faheem Ahmed, Chawki Awada, Christian Jonin, Pierre-François Brevet

Band gap engineering of Au doping and Au – N codoping into anatase TiO_2 for enhancing the visible light photocatalytic performance

Mohammed Benali Kanoun[1]*, Faheem Ahmed[2], Chawki Awada[2]**, Christian Jonin[3], Pierre-Francois Brevet[3]

[1]*Department of Mathematics and Sciences, College of Humanities and Sciences, Prince Sultan University, P.O. Box 66833, Riyadh 11586, Saudi Arabia*
[2]*Department of Physics, College of Science, King Faisal University, P.O. Box 400, Al-Ahsa, 31982, Saudi Arabia*
[3] *Institut Lumière Matière, Université de Lyon, UMR 5306 CNRS, Université Claude Bernard Lyon 1, 69622 cedex, Villeurbanne, France.*

Abstract

We investigate anatase TiO_2 doping with Au to determine the change in the band gap energy and optoelectronic properties using experimental and theoretical analysis. The structural analysis using XRD patterns revealed that the synthesized materials primarily exhibited an anatase phase of TiO_2, with no impurity peaks observed. However, as the concentration of Au increased, additional diffraction peaks corresponding to Au crystalline phases were detected, indicating successful doping. Furthermore, the crystallite size was found to decrease with increasing Au concentration. We observe that the band gap reduces through substitution of Au into the TiO_2 lattice from 3.09 eV to 2.78 eV, demonstrating the feasibility of bandgap tuning of the TiO_2 system. A redshift for Au doped TiO_2 is observed from absorption spectroscopy and optical absorption intensity using hybrid density functional theory, facilitating visible light absorption, although with potential electron-hole recombination limitations. To enhance a visible light photocatalytic activity for water splitting, we extend our work to explore the impact of N and Au codoping into TiO_2 lattice. It reveals that the combination between N and Au leads to a suitable reduction in the band gap width of pure TiO_2. Interestingly, Au-N codoping may decrease the effect of photogenerated carriers, produce a new optical absorption feature in the visible region, and enhance the photocatalytic performance of TiO_2. This codoping configuration is also a promising photocatalyst for the decomposition of water using visible light without inducing unoccupied states.

Corresponding authors: * mkanoun@psu.edu.sa, ** cawada@kfu.edu.sa

Keywords: Experimental study, first principles computations, Au doped and Au – N codoped TiO_2, band gap, optical absorption**,** photocatalytic activity

1. Introduction

During the last years, the technology of clean and renewable energy has received wide interest for the development of economic sustainability and decreasing of atmospheric and industrial pollution [1,2]. Currently, semiconductor photocatalysis is an advanced and effective method for degrading organic contaminants and solving the issue of clean energy [3]. Accordingly, photocatalytic materials have been considered for these purposes, especially semiconductor photocatalysts and have gained a lot of attention because of their excellent physical and chemical stability, high photocatalytic activity, nontoxicity, and relatively low cost [4]. Titanium dioxide (TiO_2), which is the most commonly studied photocatalyst, has a characteristic large bandgap (>3 eV) [5]. This indicates that photocatalytic performance is limited to the ultraviolet (UV) spectral region with the wavelength below 400 nm [6]. Consequently, systematic investigation has concentrated on expanding the light absorption limit of TiO_2 toward longer wavelengths [7-16]. Substitutional doping through various schemes is considered as a practical approach for controlling the optoelectronic properties and extending the functionalities of TiO_2 under visible light irradiation [17]. The nature of the dopant atom has an impact on this activity as the impurities can be incorporated as substitutional, interstitial, or both together. Various doping procedures have been utilized for fabricating doped materials such as the sol–gel process, ultrasonic treatment followed by UV irradiation, chemical vapor deposition or other commercial titania impregnation procedures [13,18-23]. Many experimental [7-14] and theoretical [15-38] investigations were reported to enhance the photocatalytic performance of TiO_2 using various dopant transition metals, alkali metals, p-block metals and nonmetals as well as noble metals. Among them, Au doping has received the most attention in the area of photocatalysis, because of the significant influence on the changes of the electronic properties of TiO_2. Nobel metal such as Au can boost visible light absorption owing to the surface plasmon resonance effect [13]. Moreover, TiO_2 nanoparticle growth and facet formation can be affected by gold dopants,

creating unusual morphologies and surface structures that can improve photocatalytic performance. The presence of Au dopants can facilitate numerous chemical processes on the TiO_2 surface, extending the potential application of material beyond photocatalysis [36-38]. Some experimental studies have reported that the Au incorporation in TiO_2 could exclude the recombination of electron/holes and yield a significantly enhanced optical absorption in the visible range [38]. It also showed from optical absorption spectrum measurements that a new peak of energy below 3.2 eV presented in Au/Au^{3+}-TiO_2 increased optical absorption characteristic in the visible range and allowed it to be activated by visible light [38]. On the theoretical side, it was revealed that Au doping into TiO_2 effectively shifts the absorption band edges of pristine TiO_2 towards the visible range, locating it in the region of 400–1000 nm [30].
Through a combination of first principles computations and several experimental analyses (FESEM, UV−vis spectroscopy, photoluminescence, Raman), in this work we analyze the modifications in morphology structures, electronic structures, and optical properties due to Au doped TiO_2. The stability of various doping states as well as the optimum growth atmosphere conditions have been demonstrated, which is useful for n-type or photocatalytic applications. We also explored the effect of Au – N codoping on the stability, electronic structure and photocatalytic performance of TiO_2. The findings suggest that Au – N codoping might have the potential to improve visible light photocatalysis.

2. Materials and methods

2.1. Experimental section

For the preparation of TiO_2, a homogeneous mixture containing 2 mL of 0.1 M CTAB solution and 30 mL of ethanol was prepared by mixing and stirring with a magnetic stirrer. After proper mixing, 1.02 mL of Ti isopropoxide (3.45×10^{-3} moles) solution was added to this mixture and then heated to 65 ^{0}C with continuous stirring. After heating and stirring for 5 min, a white precipitate appeared, which was continuously stirred and heated. After ~45 minutes, the solution becomes completely white in color. In this stage, $HAuCl_4$ with different molar fraction of 0%, 0.5% (5.86 mg), 1 % (11.7 mg), and 2 % (23.44 mg), respectively was added to the white solution to prepare pure TiO_2 and Au-doped TiO_2. Then, 50 mL of di-ionized (DI) water was added under continuous heating and stirring for 15 minutes. After, the formed solution was kept precipitating overnight. The precipitate was collected, washed several times with DI water and

ethanol, and finally centrifuged at 4000 rpm 3 times using DI water. The dried solid white mass was collected, then dried and annealed at 600 ^{0}C for 1 hour in an aerated oven. The product was then called as pure TiO_2 and Au-doped TiO_2 and was used for further characterizations. X-ray diffraction (XRD) was used to characterize the crystal structure of the prepared samples. The system consists of X-ray diffractometer (Phillips X'pert (MPD 3040)) with Cu Ka radiations (λ = 1.5406 Å) at voltage of 40 kV and a current of 30 mA. A field emission scanning electron (FESEM) microscope (JEOL-JEM) equipped with EDX has been used to study the surface topography of the synthesized powders. A confocal Raman microscope (LabRAM HR800) was used to perform the Raman measurements, and photo-electron spectra were recorded using a multichannel charge-coupled detector (CCD). Raman spectra were reported at ambient room temperature using a backscattering geometry with a spectral resolution of 0.8 cm^{-1}. For the excitation of the samples, a Helium Cadmium blue laser (wavelength 442 nm and an output power 20 mW) was used. The optical characteristics of Au –doped TiO_2 were obtained at room temperature by estimating the UV-Vis absorbance in the wavelength range [200 – 800 nm]. A spectrophotometer (Hitachi UV-3600) with an integrating sphere that enables the measurement of powder absorbance spectra.

2.2. Computational details

Using the linear combination of atomic orbitals method as basis set, the Quantum Atomistix ToolKit (QuantumATK) software package [39] was used to perform theoretical calculations based on the density functional theory (DFT) framework, within the generalized gradient approximation (GGA) exchange-correlation functional of the Perdew, Burke, Ernzerhof (PBE) [40]. The FHI pseudopotential with double zeta polarized considering the medium basis set was adopted. A mesh cutoff energy of 60 Ha is used. With a tolerance value of 10^4 Ha, the PulayMixer algorithm was used as an iteration control parameter. The structures were completely optimized utilizing the limited-memory Broyden–Fletcher–Goldfarb–Shanno (LBFGS) approach, with force on each atom position less than 0.05 eV/ Å. A 4 × 4 × 2 Monkhorst-Pack [41] k-grid was used for geometry structure optimization, while a 8 × 8 × 4 grid was applied for electronic property calculation. The Heyd-Scuseria-Ernzerhof HSE06 hybrid functional was used to calculate all of the electronic structures and optical properties [42-44].

3. Results and discussion

3.1. Structural properties

XRD patterns were investigated to present the structure and phase configuration of as-synthesized materials. The analysis of Figure 1 shows that the XRD patterns are attributed to pure TiO_2 and gold doped TiO_2. The XRD patterns show different diffraction peaks at 2θ angles 25.3, 37.9, 48.05, 53.9, 55.06, 62.4, 68.76, 70.3, 75.06 assigned to the crystal planes of the anatase phase TiO_2 [(101), (004), (200), (105), (211), (204), (116), (220), (215)] (see JCPDS card no. 21-1272). Moreover, there are no impurity peaks to be observed, only clear and sharp peaks. The latter confirms the purity of the synthesized anatase phase of TiO_2. On the other hand, samples of 0.5% and 2% doped TiO2 show some diffraction peaks at 2 angles 38.21, 44.35, 64.7, and 77.7. They belong to the crystal planes of gold (111), (200), (220), and (311), respectively, (JCPDS card No. 04-0784). A significant increase of these peaks is observed with the increase of the Au fraction. To calculate the crystallite size of all the prepared samples, we used the Debye Scherrer equation shown below [45]; $D = \frac{k\lambda}{\beta cos\theta}$, where k is a constant, λ is the X-ray wavelength, β is the full width at half maximum (FWHM) parameter and θ is the diffraction angle. It is observed that the crystallite size drops off with the rising of Au concentrations. The crystallite size of pure TiO_2, 0.5% Au-doped TiO_2, 2% Au-doped TiO_2 was found to be 52 nm, 41 nm, and 48 nm, respectively. The morphologies studied by FESEM and the EDX plots of pure and Au-doped TiO_2 nanoparticles with various doping concentration of Au were shown in Figure S1 and S2.

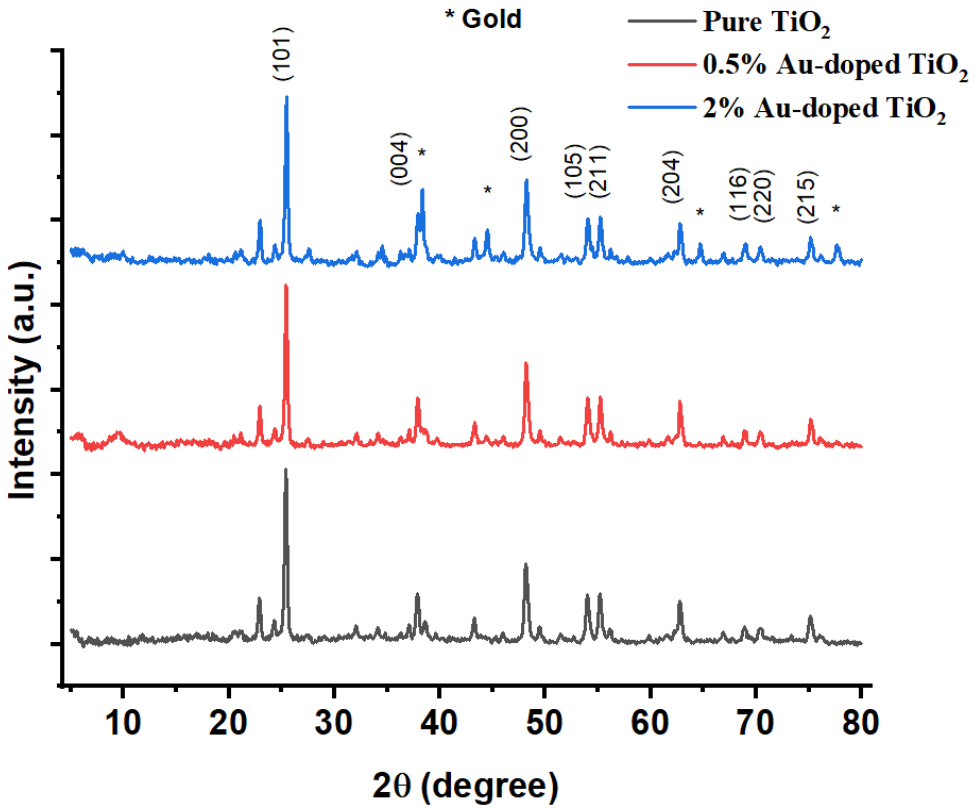

Figure 1: XRD patterns of pure TiO_2, 0.5%, and 2% Au-doped TiO_2 nanoparticles.

To support the experimental measurements of the crystal lattices, we carried out first-principles computations on hexagonal TiO_2 anatase with the space group $I4_1/amd$. The optimized lattice parameters match the experimentally reported values rather well [46], and previous theoretical works [33,34,47] as listed in Table 1. Then, based on an optimized unit cell, 2 × 2 × 2 supercells were built containing 96 atoms, as illustrated in Figure S3. The substitutional defect was created in the supercell by simultaneous replacement of a Ti atom by an Au atom (equivalent to 3.125% Au composition). The co-doped configurations were produced by simultaneously changing a Ti atom for a Au atom and an O atom for an N atom. The formation energy is computed for Au doped and Au – N codoping TiO_2 configurations according to expression; $E_f = E_{doped} - E_{undoped} - n_{Au}\mu_{Au} + n_{Ti}\mu_{Ti} + n_O\mu_O - n_N\mu_N$, where E_{doped} denotes the total energy of the doped system and dopant, and $E_{undoped}$ is the total energy of the pure TiO_2 [48,49,50]. The number of added or removed dopant and host ions is represented by n. The chemical potentials of the Au, Ti, N and O atoms, are defined by μ_{Au}, μ_{Ti}, μ_N and μ_O respectively, varying depending on the experimental circumstances. In the case of Ti-rich and an O-rich situation, μ_{Ti}

and μ_O can be obtained in the stable state with energy of bulk Ti and O_2 molecule, respectively. The relation, $\mu_{Ti} + 2\mu_O \approx \mu_{TiO_2}$, can be used to estimate the chemical potentials of Ti under O-rich environments and O under Ti-rich environments, in which μ_{TiO_2} can be thought of as the total energy per TiO_2 formula unit. The chemical potential for Au is known and calculated using the formula, $2\mu_{Au} + 3\mu_O \approx \mu_{Au_2O_3}$, where $\mu_{Au_2O_3}$ is computed from the total energy of the Au_2O_3 [47,48]. The computed formation energies for doped and codoped TiO_2 systems are gathered in Table 1. According to these findings, Au doped systems form a more energetically preferable structure in O-rich growth circumstances than in Ti-rich growth settings. In the optimized geometry structure of Au doped TiO_2, it is found that the lattice constants increase slightly with regard to that of pure TiO_2, as listed in Table 1. The doping with Au in TiO_2 shows that the tetragonal crystalline structure is distorted, resulting in this observed variation.

Table 1. The predicted lattice constants, and the formation of energy for pristine, doped and codoped TiO_2.

	a (Å)	*c* (Å)	E_f (eV)	
			Ti-rich	O-rich
Pure	3.782 (3.7842 [46])	9.496 (9.5146 [46])	-	-
Au	3.825	9.512	10.5	4.84
Au - N	3.793	9.485	12.87	3.75

3.2. UV-Vis optical absorption properties and electronic structures

UV-vis diffuse reflectance spectra (DRS) of pure TiO_2 and 0.5 and 2 % Au-TiO_2 was obtained using Kubelka-Munk equation [21], as displayed in Figure 2. Figure 2(a) shows the surface plasmon resonance owing to the collective oscillation of conduction electrons in gold nanoparticles or clusters. A band gap study was performed by plotting Tauc equation $(\alpha h\nu)^{1/2}$ versus the incident photon energy, see Figure 2(b). Regarding the structural analysis of the samples, we plotted the tauc equation with n=2 that lies to the anatase phase where the band gap is indirect. The obtained band gap values for the samples are 3.09 eV, 2.82 eV and 2.78 eV for

TiO_2, 0.5% Au-TiO_2 and 2% Au-TiO_2, respectively. The doping process reduces the band gap marginally, but still potentially increases the system photocatalytic performance.

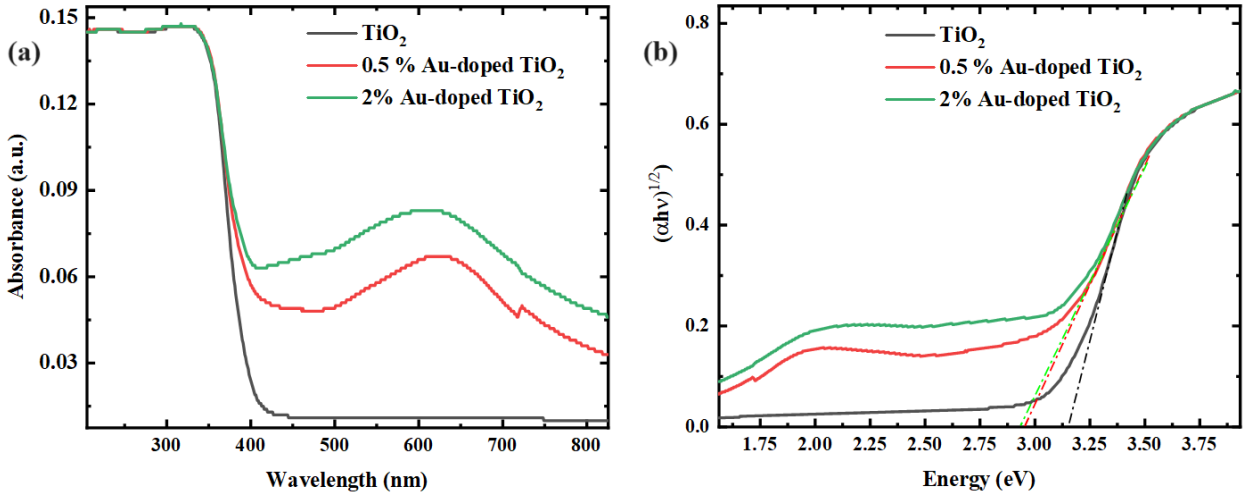

Figure 2: UV-visible absorption spectra for pure TiO_2, 0.5%, 1%, and 2 % of Au-doped TiO_2. a) Absorbance versus wavelength. b) Tauc plot of the absorbance versus incident photon energy by using indirect transition of band gap.

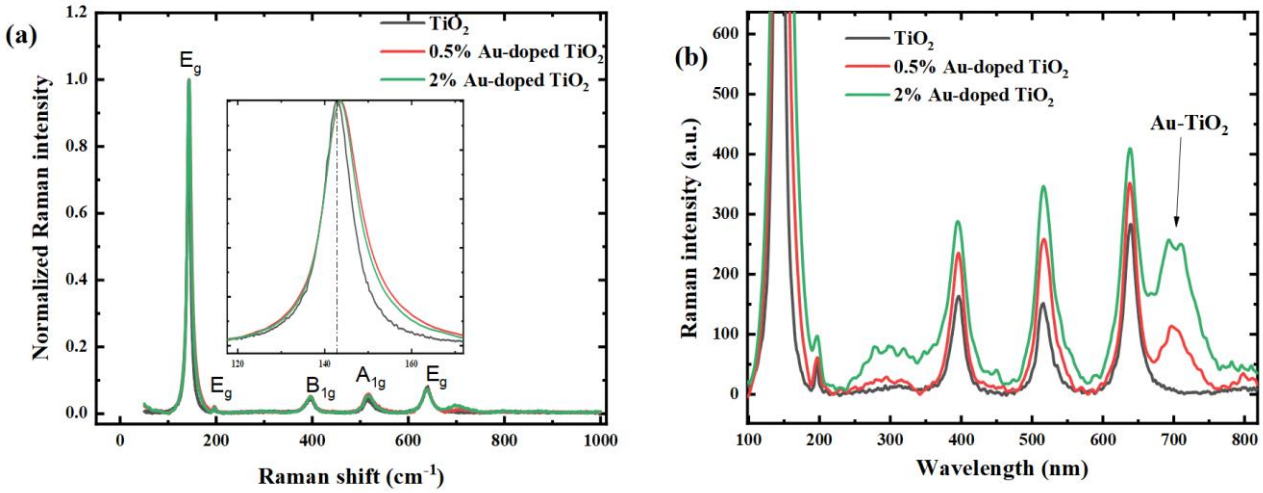

Figure 3: Raman spectra of pure TiO_2, 0.5%, and 2 % of Au-doped. Inset shows the shift and the broadening of the E_g phonon mode. b) Zoom in of the Raman spectra.

Figure 3(a) presents the Raman spectra of pure TiO_2, 0.5%, and 2% of Au-doped TiO_2. The observed phonon modes belong purely to anatase phase. This anatase phase crystallizes in tetragonal structure with a space group $I_{4_{1/amd}}$ and point group D_{2d}. The two TiO_2 units

composing the primitive cell give, six Raman–active modes in the Raman spectrum: three E_g, two B_{1g}, and one A_{1g} modes [51]. It is shown a shift toward the high vibrational energy and a broadening of the $E_g$mode resulting from the incorporation of the gold atoms into the TiO_2 matrix. In addition, a new phonon mode located at 700 cm^{-1} was observed. The latter may be assigned to the presence of a new phase of TiO_2-Au or multiphonon scattering in the disordered anatase phase because of the presence of impurities.

To explore the influence of Au doping and (Au – N) codoping on the variation of the electronic properties TiO_2, we calculated the electronic band structures and density of states (DOS) of Au-doped TiO_2 and (Au – N) codoping with pristine TiO_2 for comparison, as illustrated in Figure 4. The electronic band structure of pristine TiO_2 calculated with the HSE06 functional exhibits the upper of valence band (VB) situated at Γ- and X-points and the lower of conduction band (CB) folding at Γ-point, as shown in Figure 4(a). The band gap is found to be indirect in nature with an energy value of 3.58 eV. This is rather consistent with our obtained experimental measurements (3.09 eV) and the previously reported experimental (3.20 eV) [5] and theoretical (3.17-3.59 eV) works [18,32-34,52,53]. When incorporating Au into the TiO_2 lattice, two new impurity states emerge in the band gap region to form intermediate states just below the minimum of the CB, as displayed in Figure 4(b). It is also observed that both valence and conduction band edges are shifted to lower energies. Our results reveal that the energy separation between the edges of the VB and the CB amounts to 3.18 eV for Au-doping, indicating a reduction in the band gap width. The decreased bandgap favors the absorption of the visible region, while the non-occupied impurity features above the Fermi level act as electron-hole recombination centers and lower the photocatalytic efficiency. To avoid this limitation, the codoping N with Au into TiO_2 is investigated. As expected, Figure 4(c) demonstrates that for (Au - N)-co-doped configuration, no impurity states are observed close to Fermi level. The predicted band gap has a value of 1.71 eV.

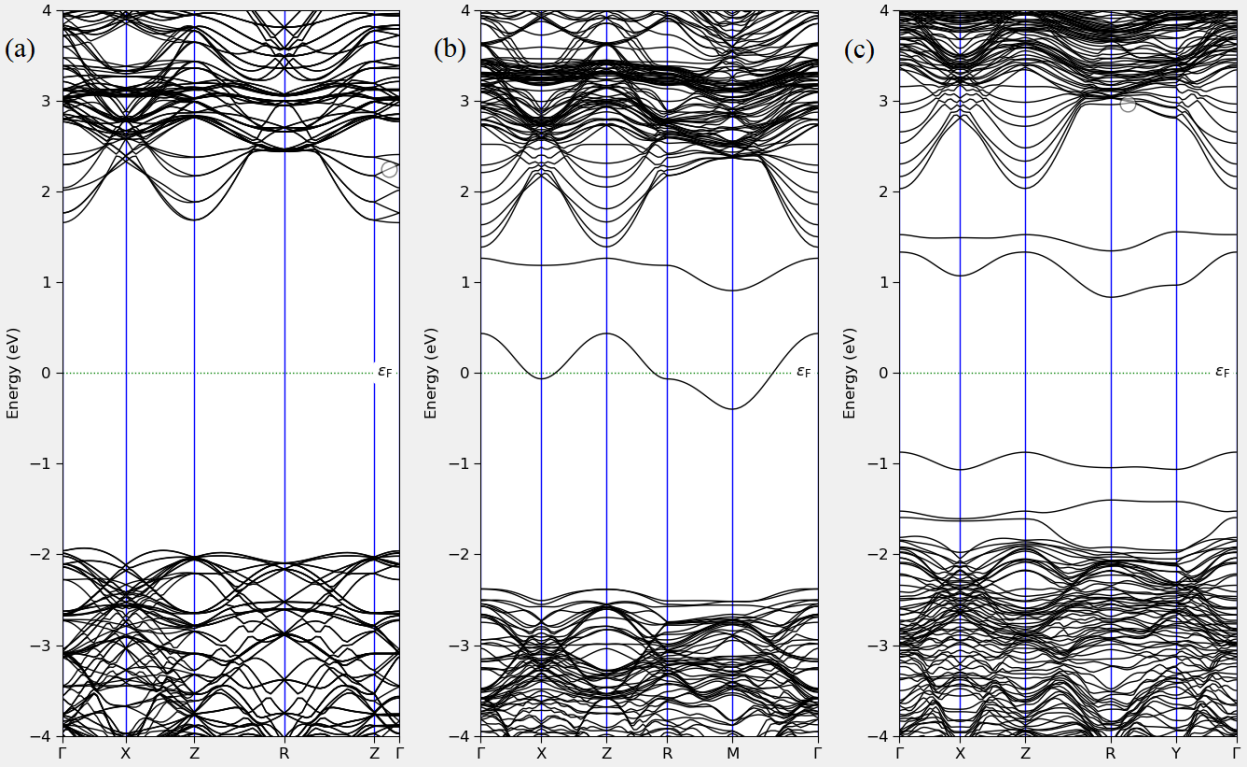

Figure 4. Calculated band structure of (a) pristine TiO_2, (b) Au doped TiO_2 and (c) (Au – N) co-doped TiO_2.

An examination of the DOS from Figure 5(a) of pure anatase shows that the edge of the VB is primarily characterized by the O 2p states, indicating that electrons in the VB are primarily localized on O atoms. While the lowermost part of the CB is mostly dominated by empty Ti 3d states, implying that in the absence of any dopants, the excited electrons are promoted from O 2p states to empty Ti 3d states during electronic transitions. For the Au doping into TiO_2, it is observed that two separate local DOS peaks emerge in the band gap with the first peak being partially occupied around the Fermi level and the second peak being unoccupied just below the CB (see Figure 5(b)). The presence of these peaks indicates the creation of new energy levels within the band gap due to Au doping. Furthermore, at roughly 0.5 eV from the minimum of the CB, a distinct Au state is added in the bandgap, demonstrating the allowed electron transitions under visible light spectrum. The Au-induced donor state has a high contribution of Au 5d states, as well as small components of O 2p and Ti 3d states, indicating that the O 2p - Au 5d hybridization has occurred. The deep Au states provide sites from which electrons can be triggered in response to light absorption. As a result, there are more charge carriers. In spite of

this, they might act as recombination sites for these charge carriers. Thus, the reaction to visible light enhances the optical absorption of Au doped TiO_2. When Au and N are combined, as shown in Figure 5(c), Ti 3d states contribute mostly to the lower part of CB, while O 2p and N 2p states make up the maximum of VB. It is also shown that the bandgap is noticeably reduced as a result of the creation of continuous bands just below the lower of the CB and above the edge of the VB. In both instances, the upper of VB is built up from hybridized O2p - N2p states, while the minimum of CB is mostly composed of Ti 3d mixed with Au 5d states. The Au cation at a Ti site provides one electron to the TiO_2 lattice, while the N dopant ion at an O site generates one acceptor level in the band gap. As a result, the (Au - N) co-doped system experiences full charge compensation, allowing the recombination centers to be eliminated. This modification allows for efficient utilization of visible light, enhancing the photocatalytic performance of the Au-N codoped TiO_2 system.

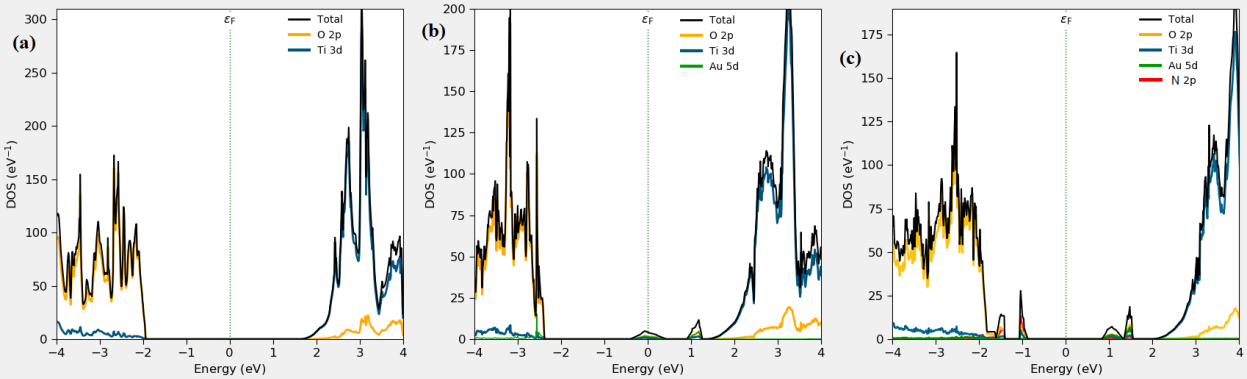

Figure 5. Calculated total and partial DOS of (a) pristine TiO_2, (b) Au doped TiO_2 and (c) (Au – N) codoped TiO_2.

To examine the absorption features in pristine, Au doped TiO_2 and (Au – N) codoping TiO_2 systems, we calculated optical absorption coefficient, as a function of the wavelength of incident light using HSE06 functional, as shown in Figure 6. The analysis of Figure 6 of pure TiO_2 reveals that it can only absorb in the UV range, with no visible range absorption response. The Au doping causes a minor red shift of the edge of absorption because of the in-gap level impurities. This small red shift is consistent with the observed experimental red shift for Au-doped TiO_2 nanoparticles, caused by a modest band gap reduction rather than gap state excitation. The augmentation of the absorption in the visible light for Au doped TiO_2 is

consistent with the excitation energy from the dopant states in the band gap to the minimum of the CB. These results indicate that the electrons could be excited from the edge of the VB to the empty gap state, resulting in a new optical absorption in the visible region. According to the absorption curve of codoping configuration indicates that when Au and N are combined, the absorption strength increases and the absorption peak extends throughout the entire visible light spectrum compared with the pure and monodoping TiO_2. The major difference here may be related to the rise of the dopant energy levels below the lower of CB and above maximum of VB in Au – N codoping as compared with those in pristine and Au doping.

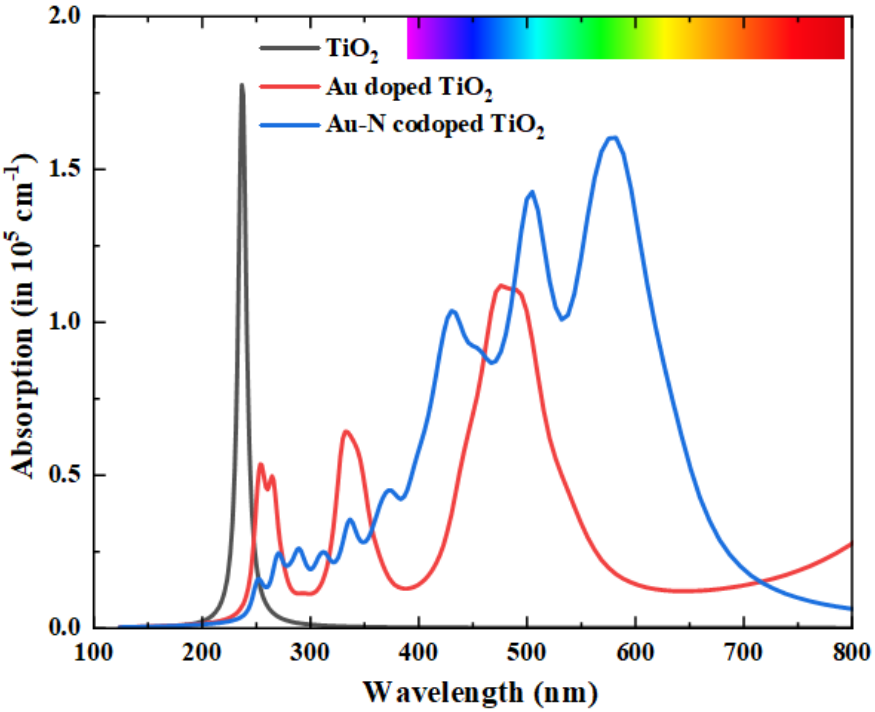

Figure 6. The absorption spectra of the pure and Au doped and (Au – N) co-doped TiO_2.

In addition to possessing the appropriate bandgap to collect visible light, the upper VB and the lower CB of a perfect water-splitting photocatalyst should be positioned correctly. Figure 7 shows the capacity of monodoping and codoping systems for photocatalytic water splitting. The calculations for the VB and CB edges, which are estimated in relation to the normal hydrogen

electrode (NHE), are described in detail in references [43,54-57] (see supporting information). The VB and CB edge positions of a desirable photocatalyst for overall water splitting must be adjusted in relation to the water redox potentials to allow for the spontaneous release of oxygen and hydrogen. From Figure 7, it can be seen that the CB and VB edge positions of pure TiO_2 are above and below the redox potential and oxidation potential of water, respectively. This is in line with prior experimental and theoretical findings [58]. Au doping results in the formation of an occupied intermediate band, which may allow charge carriers to move from the valence area to the conduction region. Furthermore, the production of hydrogen and oxygen in au doping is thermodynamically impossible. For Au-N codoping, the maximum of CB is 0.48 eV below the H/H_2 level whereas the maximum of VB is 0.96 eV below the H_2O/O_2 energy. This demonstrates that Au-N codoping only has the capacity for spontaneous oxygen generation.

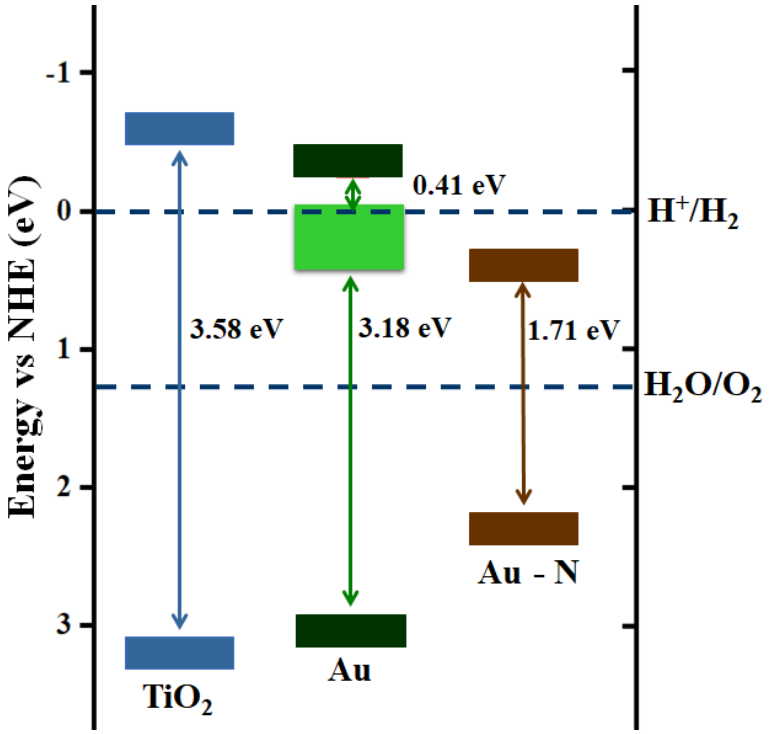

Figure 7. Schematic illustration of computed maximum of VB and minimum of CB of the pure, Au doped and Au - N codoped TiO_2 with respect to the water reduction and oxidation potentials. (The delocalized impurity bands are identified by the green)

Conclusions

A combined experimental and computational investigation was used to evaluate the structural, electronic, and optical characteristics of Au doped TiO_2, improving our understanding of the impact of Au doping into TiO_2 lattice and possibilities for enhancing their properties for visible photocatalytic performances.

The following are the main findings of our thorough analysis.

(a) The calculated formation energies reveal that Au doped TiO_2 systems form more energetically preferable structure in O-rich growth circumstances than in Ti-rich growth settings.

(b) Significant band-gap reduction is seen within the replacement of Ti by Au at small concentrations, in which new impurity states appear in the band gap region to form intermediate states just below lower of the CB, thereby displaying the n-type behavior.

(c) Increasing the Au content in TiO_2 leads to a decrease in the bandgap energy, the main origin in the observed red shift of the absorption edges, inducing an absorption coefficient peak in the visible-light spectral region.

(d) Passivated Au - N codoping in TiO_2 reveals that the combination between N and Au leads to a suitable reduction in the band gap width of pure TiO_2. Interestingly, Au-N codoping may deduce the effect of photogenerated carriers, produce a new optical absorption feature in the visible region, and enhance the photocatalytic performance of TiO_2.

This research therefore contributes to the development of ideas for improving optical absorption and photocatalytic performance in the visible light spectral domain in Au doped and Au – N codoped TiO_2 systems by providing fundamental insights into this important question.

Author Contributions

Conceptualization M.B.K., F.A. and C.A.; Data curation, F.A. and M.B.K.; Formal analysis, M.B.K., F.A. and C.A.; Funding acquisition, C.A.; Computational methodology, M.B.K. (lead), Experimental methodology, F.A. and C.A. (lead); Writing—original draft, M.B.K., F.A. and C.A.; Writing—review & editing, C.A., C.J. and P.-F.B. All authors have read and agreed to the published version of the manuscript.

Conflicts of interest

There are no conflicts to declare.

Acknowledgments: The authors extend their appreciation to the Deputyship for Research & Innovation, Ministry of Education in Saudi Arabia for funding this research work through the project number (1063).

References

[1] K. Li, B. Peng and T. Peng, Recent Advances in Heterogeneous Photocatalytic CO2 Conversion to Solar Fuels, ACS Catal, 2016, 6, 7485–7527
[2] C. Byrne, G. Subramanian and S. C. Pillai, Recent Advances in Photocatalysis for Environmental Applications, J. Environ. Chem. Eng., 2018, 6, 3531–3555
[3] F Opoku, K K Govender, C G C E van Sittert, P P Govender, Recent Progress in the Development of Semiconductor-Based Photocatalyst Materials for Applications in Photocatalytic Water Splitting and Degradation of Pollutants Advanced sustainable systems, 2017, 1, 1700006
[4] Z. Weng, H. Guo, X. Liu, S. Wu, K. W. K. Yeung and P. K. Chu, Nanostructured TiO_2 for energy conversion and storage, RSC Adv., 2013, 3, 24758–24775.
[5] D. O. Scanlon, C. W. Dunnill, J. Buckeridge, S. A. Shevlin, A. J. Logsdail, S. M. Woodley, C. R. A. Catlow, M. J. Powell, R. G. Palgrave, I. P. Parkin, G. W. Watson, T. W. Keal, P. Sherwood, A. Walsh and A. A. Sokol, Band alignment of rutile and anatase TiO_2, Nat. Mater., 2013, 12, 798–801
[6] V. Etacheri, C. Di Valentin, J. Schneider, D. Bahnemann, S.C. Pillai, Visible-light activation of TiO2 photocatalysts: advances in theory and experiments. J. Photochem. Photobiol. C: Photochem. Rev. 2015, 25, 1–29.
[7] X. Yang, Y. Min, S. Li, D. Wang, Z. Mei, J. Liang and F. Pan, Conductive Nb-doped TiO_2 thin films with whole visible absorption to degrade pollutants Catal. Sci. Technol., 2018, 8, 1357–1365.
[8] Y. Li, X. Wu, Y. Duan, Z Huang, J. Fan, S. A.C. Carabineiro, K Lv, Oxygen vacancies-induced photoreactivity enhancement of TiO_2, mesocrystals towards acetone oxidation Appl. Surf Sci 2022, 594, 153519
[9] Z. Hu, C Yang, K Lv, X Li, Q Li, J Fan, Single atomic Au induced dramatic promotion of the photocatalytic activity of TiO_2 hollow microspheres, Chem. Commun., 2020, 56, 1745-1748
[10] Z Hu, K Li, X Wu, N Wang, X Li, Q Li, L Li, K Lv, Dramatic promotion of visible-light photoreactivity of TiO_2 hollow microspheres towards NO oxidation by introduction of oxygen vacancy, Applied Catalysis B: Environmental 2019, 256, 117860
[11] X. Chen and C. Burda, The Electronic Origin of the Visible-Light Absorption Properties of C-, N- and S-Doped TiO_2 Nanomaterials J. Am. Chem. Soc., 2008, 130, 5018–5019.
[12] H. A. Hamedani, N. K. Allam, M. A. El-Sayed, M. A. Khaleel, H. Garmestani and F. M. Alamgir, An Experimental Insight into the Structural and Electronic Characteristics of Strontium-Doped Titanium Dioxide Nanotube Arrays, Adv. Funct. Mater., 2014, 24, 6783–6796.
[13] A Khlyustova, N Sirotkin, T Kusova, A. Kraev, V. Titov, A. Agafonov, Doped TiO2: the effect of doping elements on photocatalytic activity Mater. Adv., 2020, 1, 1193
[14] Li-Juan Sun, Hai-Wei Su, Di-Fa Xu, Le-Le Wang, Hua Tang, Qin-Qin Liu, Carbon hollow spheres as cocatalyst of Cu-doped TiO_2 nanoparticles for improved photocatalytic H_2 generation, Rare Metals, 2022, 41(6): 2063-2073
[15] J.-G. Ma, C.-R. Zhang, J.-J. Gong, Y.-Z. Wu, S.-Z. Kou, H. Yang, Y.-H. Chen, Z.-J. Liu and H.-S. Chen, The Electronic Structures and Optical Properties of Alkaline-Earth Metals

Doped Anatase TiO_2: A Comparative Study of Screened Hybrid Functional and Generalized Gradient Approximation, Materials, 2015, 8, 5508–5525.
[16] C. Li, Y. F. Zhao, Y. Y. Gong, T. Wang and C. Q. Sun, Band gap engineering of early transition-metal-doped anatase TiO_2: first principles calculations Phys. Chem. Chem. Phys., 2014, 16, 21446–21451.
[17] J. W. Pan, C. Li, Y. F. Zhao, R. X. Liu, Y. Y. Gong, L. Y. Niu, X. J. Liu and B. Q. Chi, Electronic properties of TiO_2 doped with Sc, Y, La, Zr, Hf, V, Nb and Ta Chem. Phys. Lett., 2015, 628, 43–48.
[18] J. Liu, M. Weng, S. Li, X. Chen, J. Cen, J. Jie, W. Xiao, J. Zheng and F. Pan, High-Throughput HSE Study on the Doping Effect in Anatase TiO2, Phys. Chem. Chem. Phys., 2020, 22, 39–53,
[19] S. Khaoulani, H. Chaker, C. Cadet, E. Bychkov, E.; Cherif, L.; Bengueddach, A.; Fourmentin, S. Wastewater treatment by cyclodextrin polymers and noble metal/mesoporous TiO2 photocatalysts. C. R. Chim. 2015, 18, 23–31.
[20] H Yu, S Li, S Peng, Z Yu, F Chen, X Liu, J Guo, B Zhu, W Huang, S Zhang. Construction of rutile/anatase TiO_2 homojunction and metal-support interaction in Au/TiO2 for visible photocatalytic water splitting and degradation of methylene blue. Int. J. Hydrogen Energy 2023, *48*, 975-990.
[21] Y Li, X Wu, Y Duan, Z Huang, J Fan, S. A.C. Carabineiro, K Lv, Oxygen vacancies-induced photoreactivity enhancement of TiO_2 mesocrystals towards acetone oxidation, Appl Surf Sci Applied Surface Science 594 2022 153519, 594, 153519
[22] P. Ribao, J. Corredor, M.J. Rivero, I. Ortiz, Role of reactive oxygen species on the activity of noble metal-doped TiO_2 photocatalysts. J. Hazard. Mater. 2019, 372, 45–51.
[23] J.F. Gomes, A. Lopes, K. Bednarczyk, M. Gmurek, M. Stelmachowski, A. Zaleska-Medynska, E. Quinnta-Ferreira, R. Costa, R. Quinnta-Ferreira, R.C. Martins, Effect of noble metals (Ag, Pd, Pt) loading over the efficiency of TiO_2 during photocatalytic ozonation on the toxicity of parabens. Chem Engineering 2018, 2, 4.
[24] Y. X. Han, C. L. Yang, M. S. Wang, X. G. Ma and L. Z. Wang, Enhancing the visible-light absorption of TiO_2 with the use of key N, Co, and Na dopant concentrations, Sol. Energy Mater. Sol. Cells, 2015, 132, 94–100
[25] C. Li, Y. F. Zhao, Y. Y. Gong, T. Wang, C. Q. Sun Band gap engineering of early transition-metal-doped anatase TiO_2: first principles calculations, Phys. Chem. Chem. Phys., 2014, 16, 21446-21451
[26] Y F Zhao, Can Li, Song Lu, Ru Xi Liu, Ji Yuan Hu, Y Y Gong, L Y Niu, Electronic, optical and photocatalytic behavior of Mn, N doped and co-doped TiO_2: Experiment and simulation J Solid State Chem. 235,160-168, 2016
[27] M. Khan, J. Xu, N. Chen, W. Cao, Asadullah, Z. Usman, D. F. Khan Effect of Ag doping concentration on the electronic and optical properties of anatase TiO_2: a DFT-based theoretical study Res Chem Intermed 2013, 39, 1633–1644
[28] M. Khan, Y. Zeng Improving the photo-response of TiO2 by tri-doping: a DFT based atomistic study, Mater. Res. Express 2019, 6, 115510
[29] Y. Wang, R. Zhang, J. Li, L. Li, S. Lin, First-principles study on transition metal-doped anatase TiO2, Nanoscale Research Letters 2014, 9, 46
[30] M. Guo, J. Du, First-principles study of electronic structures and optical properties of Cu, Ag, and Au-doped anatase TiO_2, Physica B 2012, 407, 1003–1007
[31] J. Navas, A. Sanchez-Coronilla, T. Aguilar, N. C. Hernandez, D. M. de los Santos, J. Sanchez-Marquez, D Zorrilla, C. Fernandez-Lorenzo, R. Alcantara, J. Martın-Calleja Experimental and theoretical study of the electronic properties of Cu-doped anatase TiO2, Phys. Chem. Chem. Phys**.,** 2014, 16, 3835

[32] H. H. Ibrahim, A. A. Mohamed, I. A. M. Ibrahim Origin of the enhanced photocatalytic activity of (Ni, Se, and B) mono- and co-doped anatase TiO2 materials under visible light: a hybrid DFT study RSC Adv., 2020, 10, 43092
[33] N Shahzad, A Hussain, N. Mustaf, N. Ali, M. B. Kanoun, S. Goumri-Said First principles study of the adsorption and dissociation mechanisms of H_2S on a TiO_2 anatase (001) surface, RSC Adv., 2016, 6, 7941
[34] F. Ahmed, M. B. Kanoun, C. Awada, C. Jonin, P-F Brevet, An Experimental and Theoretical Study on the Effect of Silver nanoparticles concentration on the Structural, Morphological, Optical, and Electronic Properties of TiO_2 Nanocrystals. Crystals 2021, 11, 1488
[35] L. Giordano, G. Pacchioni, T. Bredow, Cu, Ag, and Au adsorbed on TiO_2(110): cluster and periodic calculations, *Surf. Sci.*, 2001, 471, 21-31
[36] M Boronat, P Concepción, A Corma, S González, F Illas, P Serna, A Molecular Mechanism for the Chemoselective Hydrogenation of Substituted Nitroaromatics with Nanoparticles of Gold on TiO_2 Catalysts: A Cooperative Effect between Gold and the Support, *J. Am. Chem. Soc.* 2007, 129, 51, 16230–16237
[37] A. M. Sescu, L Favier, D Lutic, N. Soto-Donoso, G. Ciobanu, M Harja, TiO_2 Doped with Noble Metals as an Efficient Solution for the Photodegradation of Hazardous Organic Water Pollutants at Ambient Conditions, Water 2021, 13, 19
[38] X. Z. Li, F. B. Li, Study of Au/Au^{3+}-TiO_2 Photocatalysts toward Visible Photooxidation for Water and Wastewater Treatment *Environ. Sci. Technol.* 2001, 35, 11, 2381–2387
[39] S. Smidstrup, T. Markussen, P. Vancraeyveld, J. Wellendorff, J. Schneider, T. Gunst, B. Verstichel, D. Stradi, P.A. Khomyakov, U.G.; Vej-Hansen, et al. QuantumATK: An integrated platform of electronic and atomic-scale modelling tools. J. Phys. Condens. Matter 2020, 32, 015901.
[40] J.P. Perdew, K Burke, M. Ernzerhof, Generalized gradient approximation made simple. Phys. Rev. Lett. 1996, 77, 3865–3868.
[41] H.J. Monkhorst, J.D. Pack, Special points for Brillouin-zone integrations. Phys. Rev. B 1976, 13, 5188–5192.
[42] J. Heyd, G. E. Scuseria and M. Ernzerhof, Hybrid functionals based on a screened Coulomb potential, J. Chem. Phys., 2003, 118, 8207–8215
[43] M.B. Kanoun, A Alshoaibi, S Goumri-Said, Hybrid Density Functional Investigation of Cu Doping Impact on the Electronic Structures and Optical Characteristics of TiO_2 for Improved Visible Light Absorption, Materials 15, 5645 (2022)
[44] B Ul Haq, M B Kanoun, R Ahmed, M Bououdina, S. Goumri-Said Hybrid functional calculations of potential hydrogen storage material: Complex dimagnesium iron hydride Int. J. Hydrogen Energy, 2014, 39, 9709 -9717
[45] Z. R. Tian, J. A. Voigt, J. Liu, Large Oriented Arrays and Continuous Films of TiO_2-Based Nanotubes, J. Am. Chem. Soc. 2003, 125, 41, 12384–12385
[46] M Horn, C F Schwerdtfeger, E P Meagher, Refinement of the structure of anatase at several temperatures, Z. Kristallogr. 1972,136, 273–81
[47] M Landmann, E Rauls and W G Schmidt, The electronic structure and optical response of rutile, anatase and brookite TiO_2, J. Phys.: Condens. Matter 2012, 24, 195503
[48] CG Van de Walle, J Neugebauer, First-principles calculations for defects and impurities: Applications to III-nitrides J. Appl. Physics 2004, 95, 3851-3879
[49] C. Freysoldt, B Grabowski, T Hickel, J Neugebauer, G Kresse, A Janotti, C. G. Van de Walle First-principles calculations for point defects in solids Rev. Mod. Phys. 2014, 86, 253

[50] M.B. Kanoun, Vacancy defects- and strain-tunable electronic structures and magnetism in two-dimensional $MoTe_2$: Insight from First-Principles Calculations**.** Surfaces and Interfaces, 27, 101442 (2021)
[51] D. Bersani, P.P. Lottici, X.Z. Ding, Phonon confinement effects in the Raman scattering by TiO2 nanocrystals, Appl. Phys. Lett. 1998, 72, 73.
[52] S. Mathew, P. Ganguly, S Rhatigan, V. Kumaravel, C Byrne, S. J. Hinder, J. Bartlett, M. Nolan, S. C. Pillai, Cu-Doped TiO_2: Visible Light Assisted Photocatalytic Antimicrobial Activity, Appl. Sci. 2018, 8, 2067
[53] M. Ikram, M A Ul Haq, A Haider, J Haider, A Ul-Hamid, I Shahzadi, M A Bari, S Ali, S Goumri-Said, M B Kanoun, The enhanced photocatalytic performance and first-principles computational insights of Ba doping-dependent TiO_2 quantum dots Nanoscale Adv., 2022, 4, 3996
[54] S. Goumri-Said, M B Kanoun, Insight into the Effect of Anionic–Anionic Codoping on $BaTiO_3$ for Visible Light Photocatalytic Water Splitting: A First-Principles Hybrid Computational Study, *Catalysts*, 2022, 12, 1672
[55] G Wang, H Chen, Yang Li, A Kuang, H Yuan, G Wu, A hybrid density functional study on the visible light photocatalytic activity of (Mo,Cr)–N codoped $KNbO_3$ Phys. Chem. Chem. Phys. 2015, 17, 28743-28753
[56] J Wang, Y. Wang, YWang, X. Zhang, Y. Fan, Y Liu, Z.Yi, Role of P in improving V-doped SrTiO3 visible light photocatalytic activity for water splitting: A first – Principles study Int. J. Hydrogen Energy, 2021, 46, 20492-20502
[57] G Wang, L Zhao, S-D Guo, J Chang, B Wang, W Zhao, B Yuan, X Long, W Zhang, P Su Bandgap engineering of KTaO3 for water-splitting by different doping strategies Int. J. Hydrogen Energy 2021, 46, 38663-38677
[58] M. Sakar, R M Prakash, T-O Do, Insights into the TiO_2-Based Photocatalytic Systems and Their Mechanisms Catalysts 2019, 9, 680